Ninth Workshop on Non-linear Dynamics and Earthquake Predictions

1 - 13 October 2007

A limited power-law for the aftershock decay rate

Clement Narteau

Equipe de Geomorphologie
Laboratoire de Dynamique des Fluides Geologiques
Institut de Physique du Globe de Paris
France

Temporal limits of the power law aftershock decay rate

C. Narteau

Geology and Geophysics, Grant Institute, University of Edinburgh, Edinburgh, UK

P. Shebalin

International Institute of Earthquake Prediction Theory and Mathematical Geophysics, Moscow, Russia

M. Holschneider

Applied and Industrial Mathematics, University of Potsdam, Potsdam, Germany

[1]   We compare the aftershock decay rate in natural data with predictions from a stochastic analytical model based on a Markov process with stationary transition rates. These transition rates vary according to the magnitude of a scalar representing the state of stress and defined as the overload. Thus, the aftershock decay rate in the model is a sum of independent exponential decay functions with different characteristic times. From different shapes of the overload distribution and different expressions of the transition rates, we discuss the magnitude of the exponent of the power law aftershock decay rate and the time interval over which we can expect to observe this regime. Before and after this time interval, we show that the decay is linear and exponential, respectively. From our analytical solutions, we deduce a model of aftershock decay rate in which a power law scaling exponent and two characteristic rates emerge. One rate is a short-term linear decrease before the onset of the power law decay to account for a finite number of events at zero time, and the other one can be interpreted as an inverse correlation time, after which aftershocks no longer occur. Then, we interpret the empirical modified Omori law (MOL) and its parameters in the framework of our theoretical model. We suggest a technique to systematically estimate and interpret the temporal limits of the power law aftershock decay rate in real sequences. We approximate these temporal limits from data available from several well-known aftershock sequences and show from an Akaike Information Criteria (AIC) that, in almost all cases examined here, our model fits better the aftershock decay rate than the MOL despite a quantitative penalty for the extra parameter required. From this work, we conclude that the time delay before the onset of the power law decay may be related to the recurrence time of an earthquake. Finally, we suggest that the power law decay rates extend over longer times according to the concentration of the deformation along dominant major faults.   *INDEX TERMS: 3299* Mathematical Geophysics: General or miscellaneous; 5199 Physical Properties of Rocks: General or miscellaneous; 7230 Seismology: Seismicity and seismotectonics; 7260 Seismology: Theory and modeling

1.   Introduction

[2]   Aftershocks are smaller earthquakes resulting of perturbations of the state of stress generated by neighboring major events. For example, they are observed in laboratory experiments following macroscopic fractures [*Mogi*, 1967], in human-related activities following mine collapses [*Phillips et al.*, 1999] or nuclear explosions [*Gross*, 1996], and, of course, with only a handful of exceptions, after other earthquakes. Because an aftershock is an earthquake and because each earthquake seems to put the crust in the

conditions appropriate to the start of a new aftershock sequence, main shocks and aftershocks are difficult to separate from each other in earthquake catalogs. No consensus has been reached about the precise definition of an individual aftershock and conclusions about general properties of the seismicity may differ according to different definitions [*Knopoff*, 2000].

[3]   The origin of the aftershock frequency, and the relationships between fault properties and the shape of the aftershock decay rate motivate the systematic description of the aftershock sequences [*Kisslinger*, 1996]. For example, a relationship between the aftershock decay rate and the heat flow [*Kisslinger and Jones*, 1991], and the role of fluids in the mechanism of stress relaxation have been emphasized.

Furthermore, aftershocks may reflect structural properties of the fault zones acquired over geological timescales [*Hirata*, 1987], and/or stress concentration heterogeneities associated with rupture propagation [*Yamashita and Knopoff*, 1987]. In our work, we consider that the state of fracturing within the aftershock zone is a critical parameter [*Nanjo et al.*, 1998]. We therefore concentrate on the possible relations between the state of stress, the state of fracturing, and the range of timescales over which the aftershock sequences extend.

[4] Aftershock sequences have internal properties, and different relationships have been established, for example, between the magnitudes of the largest aftershocks, the slopes of the frequency–magnitude of the aftershocks and the sizes or the shapes of the areas they cover [*Mogi*, 1967]. The strongest observation concerns the temporal behavior of the aftershock sequences. The aftershock rates seem to follow a power law decay and a common measure of this decay is the parameter p of the modified Omori law (MOL) [*Utsu*, 1961],

$$\Lambda(t) = \frac{K}{(t + c)^p},\qquad(1)$$

where $\Lambda(t)$ is the aftershock rate at time t, K is a constant of proportionality, and c is a time constant essential to define a finite aftershock frequency at $t = 0$. Frequently, for times less than c, the counting of the aftershocks is incomplete due to the overlappings of the seismograms. In these cases, the magnitude of c may reflect more an artifact of such saturation. Hence, the question of the aftershock frequency immediately after an earthquake remains open.

[5] Since the original empirical formula suggested by *Omori* [1894] ($p = 1$ in (1)), the aftershock decay rate has been investigated all over the world [see *Utsu et al.*, 1995, and references therein]. More complex laws with additional time-dependent behaviors have been suggested [*Otsuka*, 1985; *Kisslinger*, 1993]. Different laws provide different numbers of parameters. In this case, the best fitting model can be determined by the Akaike Information Criterion (AIC) [*Akaike*, 1974; *Ogata*, 1983]. Most of the time, exponential and power law decays are simultaneously present. Thus, the aftershock rate makes a transition from a power law to an exponential decay after a characteristic timescale (otherwise, aftershocks would occur forever). This characteristic time may be described as a "correlation time" after which aftershocks cease to occur and healing dominates. In this paper, we propose a new model of aftershock decay rate with a new set of parameters. We infer these parameters from natural data in different aftershock sequences, and we compare the performance of our hypothesis to the MOL hypothesis in order to determine which is the best fit.

[6] We adopt here the same theoretical background as *Scholz* [1968a] (section 2) so this study can be considered as a logical extension of this work. In fact, because aftershock decay rates with p value ranging from 0.9 to 1.5 are frequently observed, we focus on the fluctuations of the power law decay with factors $p < 1$, $p = 1$, $p > 1$ [*Shaw*, 1993]. We are also interested in the time limits of this power law decay to tackle fundamental questions

about the beginning and the end of the aftershock sequences.

[7] In section 2, we detail our analytical approach and suggest a model of aftershock decay rate. In section 3 we apply it to the fit of real aftershock sequences and compare our model to the MOL according to an AIC. In a vast majority of cases examined here, our model outperforms the MOL despite a penalty for an increase in complexity. Finally, we explore the possibility of extracting from real aftershock sequences the temporal limit of the power law decrease. The main results of this inference are discussed and summarized in sections 4 and 5.

2. The Model

[8] During an earthquake, the slip distribution, the speed of rupture front propagation and the segmentation of the fault contribute to change the distribution of the stress on a complex network of rough and irregular fractures. Aftershocks can be described as a part of a relaxation process of the zones of high stress [*Das and Scholz*, 1981]. Thus, we concentrate on the temporal properties of aftershock sequences assuming that they are primarily controlled by the major event. We postpone the study of the magnitude and the location of the aftershocks [*Narteau et al.*, 2000], as well as the investigations of factors like postseismic deformation, cascades of aftershocks [*Ogata*, 1999; *Sornette and Sornette*, 1999] or spatial variations of the aftershock decay rate [*Wiemer and Katsumata*, 1999].

[9] Just after the main shock, the aftershock zone is modeled by a finite number of isolated and independent intact domains. Each of them is initialized to a local overload, which locally combines the state of stress and the state of strength. Schematically, if the stress exceeds the strength, the overload is positive, the surplus is eliminated through the fracturing process, and the domain will produce a unique aftershock. Therefore, under a constant state of stress, in response to an overload σ_o, we consider that the rupture initiation is the ultimate expression of the organization of fracturing at small scales. The time dependence may come from the nature of the interactions between the increasing number of microfractures and/or chemical reaction rates which control the crack growth at an atomic scale [*Das and Scholz*, 1981].

[10] Following the study of *Scholz* [1968a], we describe how the aftershocks are distributed in time according to a Markov process with stationary transition probability. In this exponential stochastic process without memory, a function λ defines the transition rate from a stable state to the rupture according to the magnitude of the overload. At any time t, the probability that an intact domain produces an aftershock during an infinitesimal time interval dt is $\lambda(\sigma_o)dt$, and $1/\lambda(\sigma_o)$ is a characteristic time indicating the period of time between the main shock and the aftershock of an intact domain. Thus, for a population of intact domains, we study the aftershocks rate $\Lambda(t)$ from the overload distribution $N(\sigma_o, t)$ and the function $\lambda(\sigma_o)$:

$$\Lambda(t) = \int_0^\infty N(\sigma_o, t)\lambda(\sigma_o)d\sigma_o.\qquad(2)$$

Because each domain produces a unique aftershock,

$$\frac{\delta N(\sigma_o, t)}{\delta t} = -\lambda(\sigma_o)N(\sigma_o, t) \tag{3}$$

From the solution of (3) and (2), we obtain

$$\Lambda(t) = \int_0^\infty \mathcal{N}(\sigma_o)\lambda(\sigma_o) \exp(-\lambda(\sigma_o)t)d\sigma_o, \tag{4}$$

where $\mathcal{N}(\sigma_o)$ is the overload distribution immediately after the major event at $t = 0$ over a population of $N_0 = \int_0^\infty \mathcal{N}(\sigma_o)d\sigma_o$ intact domains. We now examine some particular features of the aftershock decay rates calculating using (4) from different assumed shapes of the overload distribution $\mathcal{N}(\sigma_o)$ and functions $\lambda(\sigma_o)$ (Figure 1).

[11] To obtain the analytical solution, we assume simple overload distributions, specifically a uniform distribution and an exponential decay for $\sigma_o \leq \sigma_b$ (Figure 1, first column). Through this upper limit σ_b, we assume that the perturbation of the stress produced by a major event can not be infinite. Therefore, immediately after an event, the range of stress is related to the characteristics of this event and may reflect, for example, the magnitude of the main shock, the segmentation of the fault or regional properties such as the heat flow. $\lambda(\sigma_b)$ may be described as a characteristic rate constant for the domains of highest overload.

[12] To determine the shape of $\lambda(\sigma_o)$, our basic constraint is that, for a given interval of time, an increasing magnitude of the overload increases nonlinearly the probability to trigger an aftershock. Different time-dependent laws have been suggested according to different experimental settings. For example, Scholz [1968b] suggests an exponential relationship between the strength of a single crystal and the time to failure, while subcritical crack growth experiments provide power law relationships between the stress intensity factor and the crack velocity [Atkinson, 1984]. Generally, exponential works for a single crack in a periodic crystalline structure [Lawn and Wilshaw, 1975], and power law for multiple cracks in a stochastic granular medium [Main, 1999]. Furthermore, from results of rock mechanics experiments, it is difficult to distinguish between an exponential and a power law behavior due to the narrow bandwidth of stress intensities measured [Atkinson and Meredith, 1987]. Thus, we consider both possibilities of an exponential and a power law increase of the transition rates versus the magnitude of the overload (Figure 1, second column). The fracturing process is permanently competing with strengthening processes. Under a low stress these strengthening processes may dominate, and prevent rupture initiation. For small overload, we consequently adopt a different time-dependent behavior. Practically, for a sake of simplicity, we consider a fracturing threshold at $\sigma_0 = 0$. At this fracturing threshold, the transition rates switch between λ_a and 0. Below the fracturing threshold, the time required to produce an aftershock becomes infinite. λ_a may be described as a characteristic rate associated with the threshold of crack growth. Its magnitude may vary according to structural properties or timescale associated with physical and chemical processes.

[13] From these considerations, we isolate three cases that we study in more detail. These three cases are an exponen-

tial overload distribution with an exponential expression of the transition rates (Figure 1, case A, note $\sigma_a < \sigma_c$), and an uniform overload distribution with both an exponential (Figure 1, case B) and a power law expression (Figure 1, case C, note $\delta > 0$) of the transition rates. In each case, we substitute the equations presented in Figure 1 into (4) and change the variable of integration from σ_o to $\lambda(\sigma_o)t$. Finally, in every case, the aftershock decay rate is given by

$$\Lambda(t) = \frac{A(\gamma(q, \lambda_b t) - \gamma(q, \lambda_a t))}{t^q} \tag{5}$$

with $\lambda_b = \lambda(\sigma_b)$ and where

$$\gamma(\rho, x) = \int_0^x \tau^{\rho-1} \exp(-\tau)d\tau, \tag{6}$$

is the incomplete Gamma function. Nevertheless, different cases display different aftershock decay rates:

1. case A:

$$A = N_o \frac{\sigma_a \lambda_a^{\frac{\sigma_a}{\sigma_c}}}{\sigma_b}, \text{ and } q = 1 - \frac{\sigma_a}{\sigma_c}.$$

The power law decay rate corresponds to a MOL with $p < 1$ (1). If $\sigma_a \ll \sigma_c$, $p \to 1$, and the power law decay rate becomes hyperbolic (see case B). For example, this condition is met when the overload distribution flattens ($\sigma_c \to \infty$), or when the time-dependent behavior accelerates with respect to the magnitude of the overload ($\sigma_a \to 0$).

2. case B:

$$A = N_0 \frac{\sigma_a}{\sigma_b}, \text{ and } q = 1.$$

As described by Scholz [1968a], the power law decay corresponds to the Omori law ($p = 1$ in (1)).

3. case C:

$$A = N_0 \frac{\sigma_a}{\sigma_b \lambda_a^{\frac{1}{\delta}}}, \text{ and } q = 1 + \frac{1}{\delta}.$$

The power law decay corresponds to a MOL with $p > 1$ (1). If $\delta \to \infty, p \to 1$, and the power law decay rate becomes hyperbolic (see case B). Large power law exponent ($\delta > 10$) are common in subcritical crack growth experiments on geological materials [Atkinson and Meredith, 1987].

[14] Two main characteristics of (5) are a finite value at $t = 0$:

$$\Lambda(0) = \frac{A(\lambda_2^q - \lambda_1^q)}{q}$$

and a convergent integral at long times due to the finite healing/crack growth threshold. Another characteristic is that the two terms of the numerator constrain the power law decay rate. If $\lambda_a = 0$ and $\lambda_b \to \infty$ the power law decay is permanent with respect to an exponent q. If not, under the assumption that $\lambda_b \gg \lambda_a$ three major regimes emerge
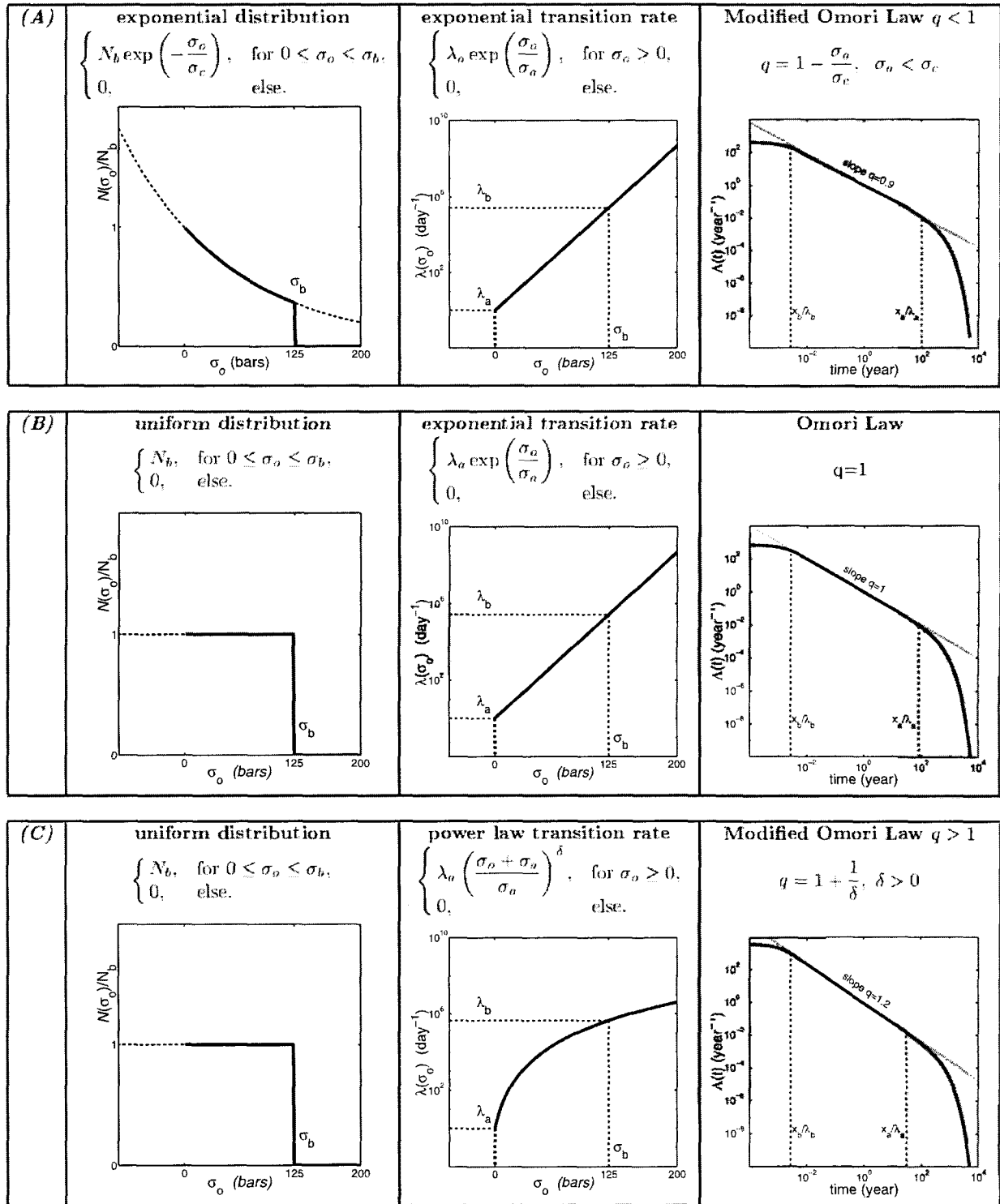
Figure 1. Different aftershock decay rates obtained from different overload distributions and different transition rates. The transition rates versus the overload are plotted in a logarithmic scale, while logarithmic scales are used for both aftershock rates and times. From (A) to (C), the power law aftershock decay rate accelerates. We determine N_b from $\int_0^\infty \mathcal{N}(\sigma_0)d\sigma_0 = N_0$. In order to illustrate the equations, we arbitrarily choose the following numerical values: $\sigma_a = 10$ bars, $\sigma_b = 125$ bars, $\sigma_c = 125$ bars, $\delta = 5$, $1/\lambda_a = 1$ day. Note that $\lambda_b = \lambda(\sigma_b)$. x_a and x_b are constants determined by a threshold of divergence between the aftershocks decay rates and a permanent power law behavior (i.e., Omori law or MOL, with $c = 0$ (1) plotted with the dotted line).
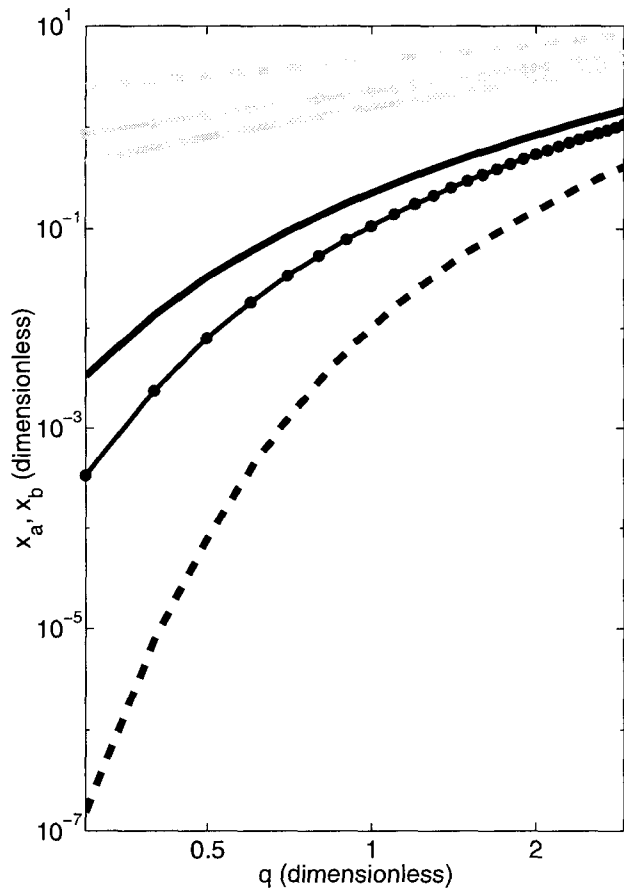
Figure 2. x_a (gray) and x_b (black) versus the magnitude of the q value for three different thresholds of divergence between the aftershock decay rate and a permanent power law decay. Logarithmic scales are used for both axes. As detailed in section 3, the divergence ζ is expressed as a percentage. In this figure, the solid, dotted, and dashed lines are for ζ values of 0.99, 0.9, and 0.8, respectively.

(Figure 1). According to a permanent acceleration of the decay rate, these regimes are,

1. a linear decay for $t < \frac{x_b}{\lambda_b}$.
2. a power law decay for $\frac{x_b}{\lambda_b} < t < \frac{x_a}{\lambda_a}$.
3. an exponential decay for $t > \frac{x_a}{\lambda_a}$.

[15] x_b and x_a are constants defined from the q value and a threshold of divergence between the aftershock decay rate and a permanent power law decay (Figures 1 and 2). In fact, the linear, the power law, and the exponential regimes are permanently present, but they dominate over different time periods. A transition time can be defined when the aftershock decay rate changes between these three regimes. These times vary according to the magnitude of q (Figure 2) and the relative magnitudes of λ_a and λ_b. If λ_b is on the same order of magnitude as λ_a, over short times, the linear, the power law and the exponential decay cannot be isolated from each other, and a transient decay persists until times greater than x_a/λ_a. Then the exponential decay dominates and it is difficult to extract from the aftershock decay rate a power law regime. This statement is also valid when σ_b tends to 0 with respect to the same power law exponent, or

when $\lambda(0)$ tends to $\lambda(\sigma_b)$ with respect to the overload distribution.

[16] In this section, we obtain a power law decay with different exponents $q < 1$, $q = 1$, $q > 1$, not only from different overload distributions but also from different expressions of the transition rates. The range of power law exponent fits with all the observations, and obviously, the parameter q may reduce to the parameter p of the MOL (1) as $\lambda_a \rightarrow 0$. Thus, the MOL is a special case of our more general model. Finally, we propose a model of aftershock decay rate (5), which we describe as the band limited power law (LPL). This LPL has both a convergent integral even with power law exponent lower than 1, and a finite value at time $t = 0$ due to the two time constants in the model. In the LPL three parameters control the decay rate: q the exponent of the power law decay and λ_a and λ_b two characteristic rates. Through λ_b and λ_a, the power law decay is limited by a linear decay over short times and a exponential decay over long times. These patterns have already been suggested and included in other formula [Utsu et al., 1995]. For example, the parameter c of the MOL for the beginning of the sequences and the Otsuka formula or the "stretched exponential" for the end of the sequences [Utsu et al., 1995; Kisslinger, 1993]. Here, our approach is not empirical and the temporal limits emerge from (1) the truncation of the overload distribution at high stress and (2) the minimum threshold of fracturing at $\sigma_0 = 0$. These follow from the requirement to avoid (1) stress singularities and (2) infinite healing times. Therefore, we do not try to justify them anymore, but focus on real data to capture such patterns, and then try to relate the properties of the aftershock decay rate to independent geophysical observations in order to validate the model. In order to do this objectively, we compare our model with the MOL hypothesis, using an appropriate statistical test in the form of the AIC.

3. Temporal Limits in Real Aftershock Sequences

[17] In addition to the aftershock sequence of the Benham (BN) nuclear test, we have investigate the temporal properties of well-known sequences of aftershocks of southern California from the Kern County event (21 July 1952) to the Hector Mine (HM) earthquake (16 October 1999) [Kisslinger and Jones, 1991; Gross, 1996]. These aftershock catalogs have been downloaded from the SCEC Data Center or provided by S. Gross.

[18] According to Gardner and Knopoff [1974], we have preliminary selected all main shocks with at least 100 aftershocks. Then, for each sequence, we have visually estimated the aftershock region from the epicenter map of the first month of aftershock activity. Most of the time, we have selected the aftershocks within circular areas, but for several earthquakes, we adopt polygonal areas in order to decrease the background seismicity rate (Table 1). Following previous works, we adopt classical techniques to measure the background seismicity rate (f), and evaluate various cutoff parameters as the minimum magnitude (M_{min}), the start time (T_{start}) and the finish time (T_{stop}) of the sequences [Utsu et al., 1995]. Thus, we consider sequences as long as possible to avoid the artifacts coming from data acquisition over short and long time periods. In order to verify that our particular selections do not affect the nature of our results,

Table 1. Characteristics of the Main Shocks and Regions of the Aftershock Sequences Studied in this Paper[a]

Main shock	Date	Latitude	Longitude	Depth	M	Aftershock Region
Imperial Valley (IV)	15 October 1979	32.63	−115.33	12	6.6	$P = (33.3, -115.6), (33.3, -115.7),$ $(32.9, -115.7), (32.6, -115.4),$ $(32.2, -115.4), (32.2, -115.0),$ $(32.3, -115.0), (32.8, -115.3)$
Oceanside (OS)	13 July 1986	32.97	−117.86	6	5.4	$R = (32.97, -117.78),$ 15 km
Big Bear (BB)	28 June 1992	34.21	−116.83	5	6.4	$R = (34.20, -116.80),$ 20 km
Hector Mine (HM)	16 October 1999	34.59	−116.27	5	7.1	$P = (35.0, -116.5), (35.0, -116.3),$ $(34.7, -116.1), (34.3, -116.0),$ $(34.3, -116.2), (34.5, -116.4),$ $(34.8, -116.5)$
Benham Nuclear Test (BN)	19 December 1968	37.25	116.48	1.4	*	*

[a]The acronym of the aftershock sequence is indicated between brackets. R indicates a circular region and P indicates a polygonal region. For the circular region, we precise the center and the radius, while for the polygonal region we precise the location of each corner.

we always compare them with the results of independent studies.

[19] From the decay rate of real aftershock sequences and the maximum likelihood procedure [Ogata, 1983], we estimate the sets of parameters of different models of aftershock decay rate. This method consists of approximating the difference between the N aftershocks occurring at times T_i, $i \in \{1,2,...,N\}$, during the time interval [T_{start}; T_{stop}] and an intensity function $\Lambda(t)$ defined from a nonstationary Poisson point process. The likelihood function is

$$L = \left\{ \prod_{i=1}^{N} \Lambda(T_i) \right\} \exp\left\{ -\int_{T_{start}}^{T_{stop}} \Lambda(t) dt \right\}, \qquad (7)$$

and allows not only to estimate the parameters of the model of $\Lambda(t)$, but also to compare different models including different number n_p of adjustable parameters via an AIC [Akaike, 1974; Ogata, 1983]:

$$AIC = 2(n_p - \max\{\ln(L)\}) \qquad (8)$$

In this optimization problem, we used the continuous minimization annealing method described by Press et al. [1992]. This minimization is slower than the downhill simplex algorithm used by Gross and Kisslinger [1994], but, avoiding local minimum, the results seem more reliable. The AIC can only be use to compare different models but does not provide information about the difference between the data and the models. In fact, for this particular problem, there is no analytical solutions for the covariation matrix of the estimated parameters [Ogata, 1983]. Then, we apply simplified estimations of errors as the Kolmogorov–Smirnov statistic and the Anderson–Darling statistic. These goodness-of-fit tests assess how well the sequence resembles to the LPL and the MOL [Press et al., 1992; Nyffenegger and Frohlich, 1998], and the results that we present have a level of confidence of at least 60%.

[20] Practically, we decompose our work in different parts. (1) We approximate and compare two independent sets of parameters: (q, λ_a, λ_b) for the LPL; (p, c) for the MOL. (2) We define the best fitting model by calculating Δ_{AIC} values, the difference between the AIC values obtained from the MOL and the AIC values obtained from the LPL. If $\Delta_{AIC} < 0$, statistically the LPL fits the data better

than the MOL despite the additional parameter. (3) For the LPL, according to different thresholds ζ, we evaluate different times t^ζ at which the aftershock decay rate diverges from the power law decay rate (Figure 2). ζ is expressed as a percentage because it measures the ratio between $\Lambda(t)$ and an idealized power law decay calculated from $\Lambda(t)$. t_1^ζ approximates the time when the linear decay is replaced by a power law decay, while t_2^ζ approximates the time when power law decay is replaced by an exponential decay. Under the assumption that $\lambda_a \ll \lambda_b$, $t_2^\zeta > t_1^\zeta$, and, t_2^ζ and t_1^ζ decreases and increases with respect to ζ respectively. (4) We interpret our results from their comparison with other geophysical observations.

[21] First, we try to demonstrate that the temporal limits of the aftershock decay rate may exist. Second, we study the origin of the magnitude of the q value. In this purpose, we are of course interested in aftershock sequences with particular patterns and we take advantage of previously published results [Kisslinger and Jones, 1991; Gross and Kisslinger, 1994; Gross, 1996]. Consequently, we only describe our results from a limited set of aftershock sequences (Table 1). These sequences are selected as a representative sample which have previously been studied in-depth (Figure 3). The aftershocks sequence are identified by acronyms related to the main shock name in order to condense the length of the text (Table 1).

3.1. The Onset of the Power Law Aftershock Decay Rate

[22] In nearly all cases, the aftershock frequencies display a non-power law decay over short times (< day), and, most of the time, it is due to the lack of events of small magnitudes [Utsu et al., 1995]. Because we now investigate the onset of the power law regime, we then have to deal with the completeness of the catalogs of aftershocks. Here, we propose to evaluate this completeness over short times by studying the evolution of the values of q, t_1^ζ, p, and c according to increasing values of M_{min}. If the q and p values stay constant, while the values of t_1^ζ and c decrease, the same power law decay appears faster for larger magnitude events [Utsu et al., 1995, Table 1 and Figure 2]. In this case, the linear decay is certainly due to incomplete catalogs, even if we can not completely eliminate other explanations related to the rupture nucleation process or the fracture size distribution. On the other hand, an increase of the c value with respect to increasing value of M_{min} has never been
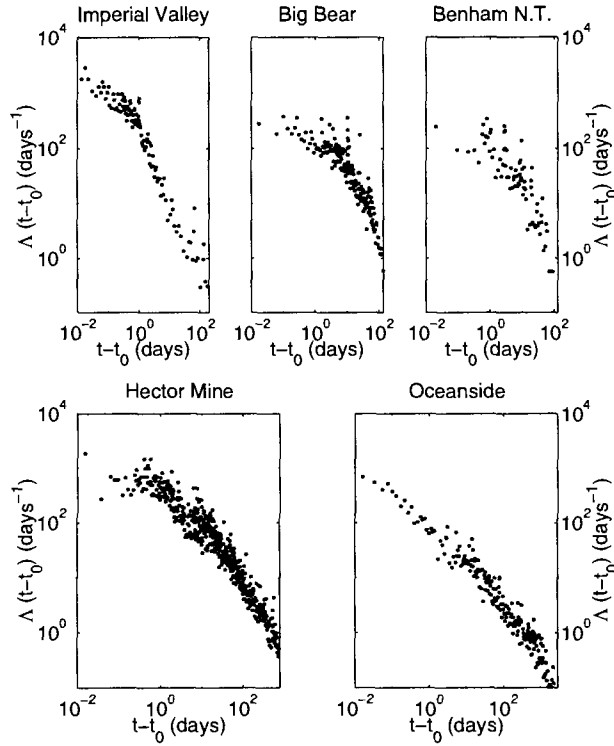
Figure 3. Aftershock decay rates for the aftershock sequences studied in this paper. $M_{min} = 2$ and t_0 is the main shock time. If t_i is the time of the ith aftershock and k a number of successive aftershocks, each dot is located at $\left(\frac{t_{i+k}-t_i}{2}, \frac{k}{t_{i+k}-t_i}\right)$.

reported, and our experiments also never show such an increase for the t_1^{ς} value. Finally, if the values of q, c, t_1^{ς}, and c stay constant, the power law decay emerges at the same time whatever the value of M_{min}. If these values of t_1^{ς} and c are not zero, it provides a solid argument for the existence of non-power law decay at the beginning of the aftershock sequences.

[23] In Table 2, we present and compare results from the modeling of the aftershock sequences of the October 1979, $M_L = 6.6$ Imperial Valley (IV) main shock, and of the October 1999, $M_w = 7.1$ HM main shock. For both sequences, we vary the value of M_{min} from 2 to 4 by step of magnitude of 0.2, and the t_1^{ς} value is calculated at $\varsigma = \{0.8;0.9;0.99\}$. The HM is a complex aftershock sequence but very well constrained from the seismological point of view. Here, we only use this sequence to underline a particular aspect of many aftershock sequence over short times. As shown by *Gross and Kisslinger* [1994], there is an active background seismicity during the IV, and we also obtain a better fit of the aftershock sequences with the addition of a constant term in the MOL (and the LPL) until $M_{min} = 3.4$. This background seismic noise has an amplitude of approximately 0.05 events d^{-1} (~18 events yr^{-1}). For magnitudes larger than 3.4, no background seismicity is required to obtain the better fit. This is always the case for the HM whatever the value of M_{min}. For the IV, because the aftershocks are clustered in space, we also study the internal properties of the subsequences of aftershocks associated with these clusters.

[24] For the IV and the HM, we can notice that values of q and p have similar high magnitudes, and that they are very stable with respect to the M_{min} value. We also observe that there are clear correlations between the variations of the values of t_1^{ς} and λ_b, and between the variations and the magnitude of the c value and the t_1^{ς} value. As expected from

Table 2. Simultaneous Comparisons Between the Aftershock Sequences of the IV Earthquake and of the HM Earthquake and Between the LPL and the MOL[a]

			LPL					MOL			
M_{min}	N	λ_b	$t_1^{0.8}$	$t_1^{0.9}$	$t_1^{0.99}$	q	f_L	p	c	f_M	Δ_{AIC}
IV (15 October 1979; $M = 6.6$, $T_{start} = 10^{-3}$ days, $T_{stop} = 200$ days)											
2.4	801	5.83	0.38	0.51	0.94	1.43	0.257	1.61	0.286	0.257	1.0
2.6	647	5.96	0.40	0.54	0.97	1.58	0.157	1.78	0.299	0.158	−1.1
2.8	470	6.74	0.38	0.51	0.90	1.7	0.098	1.93	0.28	0.099	−0.8
3.0	317	7.58	0.34	0.46	0.80	1.73	0.056	1.95	0.244	0.057	−0.4
3.2	212	6.24	0.45	0.59	1.02	1.87	0.034	2.24	0.366	0.034	−1.9
3.4	127	7.69	0.36	0.47	0.81	1.82	0.019	2.07	0.251	0.020	−2.9
3.6	68	7.35	0.33	0.44	0.79	1.59	−	1.67	0.191	−	−4.8
3.8	42	6.13	0.43	0.57	1.00	1.74	−	1.86	0.276	−	−3.7
4.0	26	6.92	0.37	0.48	0.86	1.67	−	1.78	0.229	−	−0.8
HM (16 October 1999; $M = 7.1$, $T_{start} = 5 \times 10^{-3}$ days, $T_{stop} = 800$ days)											
2.4	2557	1.21	1.49	2.09	4.04	1.14	−	1.27	1.25	−	−4.10
2.6	1657	1.62	1.16	1.61	3.08	1.19	−	1.29	0.84	−	−6.71
2.8	1130	2.38	0.79	1.10	2.10	1.19	−	1.29	0.57	−	−1.50
3.0	726	3.38	0.55	0.77	1.47	1.19	−	1.28	0.40	−	5.23
3.2	462	5.41	0.33	0.47	0.91	1.14	−	1.28	0.30	−	9.21
3.4	289	11.19	0.15	0.21	0.42	1.05	−	1.31	0.19	−	−0.84
3.6	168	27.07	0.06	0.09	0.18	1.09	−	1.27	0.08	−	−1.63
3.8	117	62.75	0.03	0.04	0.07	1.04	−	1.21	0.04	−	−4.05
4.0	77	197.87	0.01	0.01	0.02	1.00	−	1.15	0.02	−	−5.07

[a]N is the number of aftershocks for the minimum magnitude M_{min}. λ_b has units of d^{-1}, $t_1\varsigma$ and c have units of days, and q and p are unitless. Δ_{AIC} is the difference between the AICs of the LPL and of the MOL with or without a seismicity background rate according to the better fit. f_L and f_M are the seismicity background rate for the LPL and the MOL, respectively. They have units of events d^{-1}.

section 2, these observations confirm that c and λ_b are similar ingredients in the MOL and the LPL respectively. For constant q value, these observations also support that the onset time of the power law decay is closely related to λ_b, the aftershock frequency (i.e., transition rate) associated with the zone of highest overload.

[25] From the comparison of IV and HM, we observe different variations of the t_1^ζ value (i.e., c value) in response to an increase of the value of M_{min}. For the IV, the t_1^ζ value is almost constant, while for the HM, it decreases of more than 2 orders of magnitude. Therefore, in the case of the HM, we conclude that the aftershock power law decay starts rapidly (<1 hour), and that the large value of c is an artifact. On the other hand, in the case of the IV, we conclude that the aftershock power law decay starts only after few hours (between 6 and 18 hours). This time interval is consistent with other similar studies based on the observations of aftershock sequences in Japan [*Yamakawa*, 1968] or China [*Utsu et al.*, 1995]. Thus, we have the confirmation that the onset of the power law aftershock decay rate may be not the main shock time.

[26] Interestingly, in addition to the background seismicity, two particular observations characterize the Imperial fault. First, the heat flux in the region where is located the Imperial fault is high [*Lachenbruch et al.*, 1985]. *Kisslinger and Jones* [1991] noted that the high p value may be related to this heat flux. Second, the Imperial fault ruptured in 1940 during the El Centro earthquake ($M = 6.9$). The El Centro earthquake extended more toward the south along the Cerro Prieto fault, but along the Imperial fault, the surface ruptures and the offsets were similar in 1940 and in 1979 [*Sieh*, 1996].

[27] For the El Centro earthquake aftershock sequence, we find that $q = 1.02$, $\lambda_b = 30$, $t_1^{0.8} = 0.05$ days, $p = 1.02$, and $c = 0.04$ days. Unfortunately, the size of the catalogue prevents from the calculation at different value of M_{min}. Almost 40 years later, a cluster of the IV was located close to the epicenter of the El Centro earthquake. For this cluster, we find a q value lower than for the other subsequences, a larger t_1^ζ value, but, one more time, the limited number of events (16 for $M_{min} = 2.9$, $q = 1.3$, $t_1^{0.8} = 0.08$) limits the conclusion that we can draw, as well as the comparison with the value suggested by *Gross and Kisslinger* [1994]. Therefore, there is no clear evidence of variations of the power law exponent between the El Centro aftershock sequence and the IV. If there was some evidence, that should have been a possible origin of the change of the duration of the non-power law decay at short times.

[28] Theory predicts a finite delay whose duration is shorter when the crust contains zones of high overload. The data show a longer time delay, implying the absence of zones of very high overload. This absence of zones of very high overload may result from a very low preexisting stress due to the occurrence of the El Centro earthquake only 40 years before and the quasi permanent background seismic rate. In addition, through thermally activated process of stress relaxation, the amplitude of the heat flow may also limit the amplitude of the preexisting stress, and in return the magnitude of the overload. In 1940, without extrapolation on the preexisting stress and on the heat flow, a larger stress perturbation produced by a larger earthquake may explain the smaller time interval for the onset of the power

law decay rate. In the discussion, we generalize this conclusion to the properties of the aftershock sequence according to the recurrence time of earthquakes.

[29] Finally, we can see from the Δ_{AIC} value, that, even if these sequences have many different properties, the IV and HM are better fitted by the LPL than by the MOL, with only few exceptions as M_{min} is tuned. For the IV, this may be explained mainly by a better fit at the beginning of the sequence given the different shapes of the LPL and of the MOL over short times. For the HM, the origin of the better fit is discussed in the next section.

3.2. From a Power Law to an Exponential Aftershock Decay Rate

[30] In this section, we investigate the possible transition from a power law to an exponential aftershock decay rate. This transition may occur over long times and we may have to deal with low aftershock rates. Consequently, it is frequently impossible to distinguish such a transition if this transition has not been completed before the aftershock rate approaches the same order of magnitude than the background seismicity rate. This is for example the case for the IV.

[31] As described by *Gross and Kisslinger* [1994], the aftershock sequence of the July 1986, $M_L = 5.3$, Oceanside main shock (OS) is a typical example of low background seismicity rate. Moreover, these authors obtain a better fit of the OS with a so-called stretched exponential including an exponential decay over long times [*Kisslinger*, 1993]. Therefore, the OS is an opportunity of testing the LPL and of determining the superior temporal limit of the power law aftershock decay rate.

[32] In Table 3, we explore the OS by evaluating t_2^ζ, $\zeta = \{0.8; 0.9; 0.99\}$, according to different values of M_{min}. Simultaneously, we compare with the MOL. In the OS, the evolution of the c value with respect to M_{min} indicates that the power law decay is present at short times. The q and p values are less than one and reflect a slow aftershock decay rate. The λ_a values indicate a relatively low characteristic frequency. Nevertheless, because the t_2^ζ values are several orders of magnitude lower than T_{stop}, we conclude that, at this time, the exponential aftershock decay rate has become the dominant regime. This conclusion is confirmed by the magnitude and the sign of the Δ_{AIC} values, which clearly indicate that the LPL fits better the OS than the MOL. In fact, because both the ratio between the c and T_{stop} values tends to zero and the ratio between the q and p values is closed to one, the Δ_{AIC} values can only be explained by a better fit of the transition from a power law to an exponential decay rate and from the exponential decay itself. Therefore, we have verified that the transition from a power law to an exponential decay exists at least in this data set. For q value less that one, it ensures a finite number of aftershocks at infinite time.

[33] As said above, for practical reasons related to the aftershock decay rate and the background seismicity rate, most of the time, the characteristic rate has to be high to be observed. In the case of the OS, a low value can be observed because this aftershock sequence is one of the largest recorded in California for a $M_L < 5.5$ main shock. This high number of events has been explained by the low stress drop of the main shock [*Hauksson and Jones*, 1988] or the

Table 3. Transition From a Power Law to an Exponential Decay for the Aftershock Sequence of the OS Earthquake and Comparisons Between the LPL and the MOL[a]

M_{min}	N	$10^5 \lambda_a$	$t_2^{0.8}$	$t_2^{0.9}$	$t_2^{0.99}$	q	p	c	Δ_{AIC}
				LPL				MOL	
		OS (13 July 1986; $M_L = 5.3$, $T_{start} = 10^{-3}$ days, $T_{stop} = 3 \times 10^3$ days)							
2.2	1326	57	141.5	48.4	1.5	0.66	0.86	0.117	−124.67
2.4	737	58	144.2	49.8	1.6	0.67	0.83	0.033	−83.31
2.6	410	56	169.0	60.8	2.2	0.70	0.83	0.007	−43.45
2.8	249	48	197.0	71.2	2.7	0.71	0.82	0.021	−19.33
3.0	158	54	170.6	61.1	2.2	0.70	0.81	0.004	−15.08

[a]N is the number of aftershocks for the minimum magnitude M_{min}. λ_a has units of d^{-1}, t_2 and c have units of days, and q and p are unitless. Δ_{AIC} is the difference between the AICs of the LPL and of the MOL.

low seismic release of the entire aftershock sequence [*Astiz and Shearer*, 2000].

[34] In the model developed in section 2, the magnitudes of t_2, λ_a, and q are closely related to each other, but, in order to study the origin of the transition from a power law to an exponential aftershock decay rate, the magnitude of λ_a is the key parameter. This characteristic rate indicates the largest timescale of the aftershock sequence. Indirectly, it approximates the intensity of the strengthening process associated with, for example, reaction-transport mechanisms or mechanical process acting on the state of strength. Because we consider that all these processes depend on too many factors, which are difficult to dissociate from each other, we only study under what range of conditions such a characteristic rate may appear. We now explore possible relationships between the magnitude of the characteristic rate and independent geophysical observations.

[35] The OS occurred in the inner continental borderland, offshore southern California at the southern end of the Santa Catalina fault and at the northern end of the San Diego through fault [*Hauksson and Jones*, 1988; *Pacheco and Nábêlek*, 1988]. Between these two main geologic structures, the strike of the faulting curves clockwise toward the north. These fault systems seem to essentially accommodate strike-slip motions but compressive and extensive motions are also present. For example, the focal mechanisms of the largest aftershocks of the OS show reverse and strike-slip faulting [*Astiz and Shearer*, 2000]. Even if they disagree on the orientation of the fault plane of the OS event, all seismological studies suggest complex faulting patterns for this aftershock sequence. Inspired by results from laboratory test experiments and geomorphological studies detailed in section 4 [*Hirata*, 1987; *Nanjo et al.*, 1998], we focus on this possible diversity of the faulting patterns to explain the magnitude of λ_a. In fact, we test the hypothesis that the preexisting fault network constrains the aftershock decay rate. Precisely, we argue that, when the aftershock sequence is located in a region in which it is difficult to extract either a specific fault orientation or a dominant faulting mechanism, the transition from a power law to an exponential decay rate occurs at a higher aftershock frequency and consequently over shorter times. This is for example the case in regions within which no major fault exists or at the boundary between larger scale fault systems. Then, the characteristic rate at which the transition occur reflects structural property related to both the diversity of the faulting and the

correlation length of the fracturing process (i.e., the maximum length of faults). Thus, the correlation time is related to the preexisting correlation length of the stress field. Due to the possible mislocation of the aftershocks associated with the offshore location of the OS and the low value of λ_a, this hypothesis has to be validated by other observations, and, as in the previous section, we now use the HM to test our hypothesis.

[36] As said above, the HM is a complicate aftershock sequence but very well constrained by seismological observations [*Hauksson et al.*, 2002]. Once again, we extract a robust feature and confirm that the power law decay of the HM is difficult to interpret. For the HM, the surface rupture, and both the location and the mechanism of the aftershocks support a partition of the aftershock sequence. We decompose the HM in three zones delimited from the north to the south by the 34.75°N and the 34.48°N latitudes, respectively. Thus, we isolate different zones with different properties. As shown by *Hauksson et al.* [2002], the aftershocks of the southern and central zones are mostly associated with fault planes oriented following both a N6°W and a N30°W trends. The focal mechanisms of the largest aftershocks ($\geq M_L = 4.5$) are essentially strike-slip while the focal mechanisms of the smallest are more diverse. Of course, the aftershocks within these zones may reveal an increasing complexity as far as they are described in more detail but, from our point of view, they are simple. In fact, these aftershocks are confined along major fault planes which accommodate the rotating condition imposed by both the dextral strike-slip motions along these fault planes and the regional stress field [*Ron et al.*, 2001]. On the other hand, in the northern zone, *Hauksson et al.* [2002] notice that aftershock focal mechanisms are more complex, including not only strike-slip events with a larger variety of fault strike but also normal faulting. In addition, this diversity is also present in the spatial distribution of the aftershocks, in the preexisting fault network, and in the surface ruptures associated with the main shock [*USGS and CDMG*, 2000].

[37] In Table 4, we evaluate the parameters of the LPL and the MOL as well as $t_{\{1,2\}}^{0.8}$ for the three subsequences of the HM according to different values of M_{min} starting at $M_{min} = 2.6$. The comparisons between LPL and the MOL is done via the Δ_{AIC}. Only sequences with more than 40 events are taken into account and all the results can be generalized until values of $T_{start} < 16$ days. As observed by *Wiemer et al.* [2002], the fluctuations of both the p and the q values indicate that these results are not very stable. Therefore, the power law decay of these subsequences are less

Table 4. Transition From a Power Law to an Exponential Decay For the Three Subsequences of the HM Main Shock Aftershock Sequence and Comparisons Between the LPL and the MOL[a]

M_{min}	N	LPL					MOL		
		$10^5 \lambda_a$	λ_b	$t_1^{0.8}$	$t_2^{0.8}$	q	p	c	Δ_{AIC}
			HM Nord (16 October 1999; $M_w = 7.1$, $T_{start} = 5 \times 10^{-3}$ days, $T_{stop} = 800$ days)						
				North of 34.75°N					
2.6	210	277	19.4	0.032	4.4	0.39	and 1.36	19.4	−17.17
2.8	137	243	19.4	0.042	13.0	0.50	and 1.00	2.75	−13.70
3.0	89	210	28.5	0.031	19.3	0.53	0.80	0.16	−8.57
3.2	53	295	31.8	0.030	19.1	0.59	0.85	0.09	−7.38
				North of 34.48°N South of 34.75°N					
2.6	381	7	14.4	0.098	2230	0.88	0.89	0.04	−3.39
2.8	262	*	15.9	0.096	*	0.95	0.95	0.04	−3.31
3.0	176	*	17.6	0.093	*	1.03	1.02	0.03	−2.74
3.2	112	*	23.6	0.073	*	1.09	1.09	0.02	−1.43
3.4	69	*	18.1	0.110	*	1.27	1.29	0.05	−0.91
				South of 34.48°N					
2.6	114	*	11.1	0.138	*	0.96	0.96	0.059	−0.38
2.8	79	*	14.8	0.109	*	1.00	1.00	0.044	0.45
3.0	47	*	16.3	0.107	*	1.10	1.11	0.051	1.16

[a]N is the number of aftershocks for the minimum magnitude M_{min}. The star symbols indicate that our estimations of λ_a are equal to the lowest value allowed by our computations (10^{-9}). λ_a and λ_b have units of d^{-1}, $t_1^{0.8}$, $t_2^{0.8}$, and c have units of days, and q and p are unitless. Δ_{AIC} is the difference between the AICs of the LPL and of the MOL.

constrained than the one of the entire sequence (see Table 2). Nevertheless, we point out that in the northern zone, the λ_a values are high while they tend to zero in the southern zones. Furthermore, the λ_a values are more stable than the q value and the fluctuations of these two parameters are not related to each other. The $t_2^{0.8}$ value are more than 1 order of magnitude smaller than T_{stop}. Moreover, the variation of the Δ_{AIC} value indicates that the LPL fits better the northern zones of the HM than the MOL, while in the southern zones the better fit is obtained by the MOL. These results suggest that the transition from a power law to an exponential decay has been completed in the northern zone, and that such a transition is impossible to distinguish in the southern regions.

[38] Once again, we argue that the onset of an exponential decay in the northern zone may be related to different characteristics of the fault network. Interestingly, in addition to the spatial distribution of the aftershocks, larger scale geological structures can also provide supplementary evidence. The northern zone of the HM is located at the boundary between two sets of conjugate strike-slip faults. The dextral fault system extends in a N30°W direction and includes the fault segments which have ruptured during the Landers sequence and the HM earthquake, while the sinistral fault system is located more NE and extends in a N70°E direction. At the boundary between these fault systems, no major structure emerges and as shown by the April 1947, Manix earthquake ($M_L = 6.2$) sequence [Doser, 1990], it is difficult to dissociate left-lateral and right-lateral motions. Therefore, we conclude that, in the northern zone of the HM, the transition from a power law to an exponential decay is closely related to the lack of major fault and the partition of the deformation between dextral and sinistral faulting.

[39] A subsequence of HM and the OS show similar transitions from a power law to an exponential decay. They are both located at the boundary between larger fault systems and characterized by the diversity of the focal mechanism of their larger events. More indices of such a

relationship between the morphology of the fault systems and the aftershock decay rates are presented in section 3.3 and discussed in section 4.

3.3. A Transient Power Law Aftershock Decay Rate

[40] In this section, we explore another regime of aftershock sequences in order to describe additional advantages of the LPL and validate previous hypothesis.

[41] Only 3 hours after the 28 June $M_w = 7.3$ Landers earthquake, its largest aftershock was the $M_w = 6.2$ Big Bear (BB) earthquake. Given the distance from the Landers rupture (~35 km) and the magnitude of this event, the BB aftershock sequence can be treated as an independent subsequence. In this region, the seismic background is relatively high but does not improve significantly the fit of this aftershock sequence. In Table 5, we explore the BB by evaluating the parameters of the MOL and the LPL as well as $t_{\{1,2\}}^{0.8}$ according to different values of M_{min}. The variations of the c and $t_1^{0.8}$ values indicate that the power law decay is present over short times. The λ_a values are high and associate with low values of $t_2^{0.8}$ which reveal that the transition toward an exponential decay is completed only a couple of weeks after the BB earthquake. Consequently, the time delay $t_2^{0.8} - t_1^{0.8}$ is short and the power law decay is a transient regime toward the exponential one. The Δ_{AIC} values are negative while the p and q values are more and less than one respectively. Therefore, the faster power law decay shown by the MOL can be explained by a slower power law decay undergoing a transition toward an exponential decay over short times.

[42] The temporal description of the BB and the northern sequence of the HM have many things in common. Seismological and regional tectonic studies provide other similarities [Hauksson and Jones, 1993]. For example, the largest events of the BB exhibit different focal mechanisms and this sequence is decomposed in different clusters of aftershock including subparallel left-lateral faults, which have never been mapped before. From our point of view, the most important is that the BB region is also a boundary

Table 5. Transient Regime Toward an Exponential Decay Rate of the Aftershock Sequence of the BB Main Shock and Comparisons Between the LPL and the MOL[a]

M_{min}	N	$10^3\,\lambda_a$	λ_b	$t_1^{0.8}$	$t_2^{0.8}$	q	p	c	Δ_{AIC}
				LPL				MOL	
			BB (28 April 1992; $M_w = 6.2$, $T_{start} = 5 \times 10^{-3}$ days, $T_{stop} = 150$ days)						
2.8	409	18	9.51	0.13	6.07	0.75	1.24	0.51	−23.00
3.0	273	14	15.37	0.09	9.78	0.82	1.12	0.18	−12.82
3.2	200	14	18.81	0.08	11.87	0.88	1.13	0.12	−7.70
3.4	132	15	38.37	0.04	10.57	0.87	1.10	0.06	−4.23
3.6	87	15	49.10	0.03	12.94	0.94	1.10	0.03	−2.83

[a]N is the number of aftershocks for the minimum magnitude M_{min}. λ_a and λ_b have units of d^{-1}, $t_1^{0.8}$, $t_2^{0.8}$, and c have units of days, and q and p are unitless. Δ_{AIC} is the difference between the AICs of the LPL.

between two major fault systems. In fact, the BB region is limited on the north by a major thrust, and on the south by the San Andreas fault system. In addition, the recent seismicity suggests that the deformation is partitioned between thrust and more active strike-slip faults [*Webb and Kanamori*, 1985]. As before, we propose that this partitioning and the lack of dominant fault explain the high aftershock rate at which the power law decay disappear in a faster exponential decay. Such a transition can also be observed under different geophysical contexts at lower deformation rate.

[43] The earthquake activity after a nuclear explosion may be treated as an aftershock sequence since the explosion also perturbs the preexisting stress field. Such a sequence was recorded following the BN underground nuclear test on December 1968 [*Hamilton and Healy*, 1969]. Table 6 summarizes the fits of the LPL and the MOL and evaluate the best fitting model via the Δ_{AIC} according to different values of M_{min}. Our result show that the LPL fits better the BN than the MOL and confirm that an exponential decay rate is a major ingredient of the aftershock decay rate of this nuclear test [*Gross*, 1996]. Under this condition, the high p values only indicate that the MOL is unable to deal with this faster decay. The power law decay measured by the LPL is extremely slow (<0.5) but the main result resides in the magnitudes of the characteristic rates. The magnitude of λ_b tends to infinity while the magnitude of λ_a is high. Then, when they do not only reflect the overlapping of the seismogram (~6 hours according to *Hamilton and Healy* [1969]), the $t_1^{0.8}$ values tends to zero. This observation may be related to the difference between the mechanisms of a detonation and the physics of the earthquake. A detonation unlike a rupture propagation is an instantaneous and predetermined perturbation of the state of stress. Then, for nuclear tests,

zones of higher overload may exist because they can not be associated with the main event. On the other hand, the $t_2^{0.8}$ values are always lower than 30 hours and indicate that the transition toward the exponential decay is almost immediate. Supported by seismological and geodetic studies, we emphasize that this observation is again related to the morphology of the fault network but also to the magnitude of the regional stress field. First, the focal mechanisms of the largest aftershocks are partitioned between right lateral strike-slip and dip-slip, and, as proposed by *Hamilton and Healy* [1969], this diversity appear to respect the regional motions. Second, the strain rate is relatively low in this region and we consider that, in average, this region is far from failure (i.e., higher crustal strength). Thus, both the partitioning of the deformation and the low magnitude of the strain may produce a rapid transition toward an exponential decay. In this case, the power law decay is a transient state, and the MOL can not be reasonably used to model such a sequence.

4. Discussion

[44] From a restricted formalism and different examples, we have developed and tested a model of aftershock decay rate. This is a static model which describe the entire sequence from a state defined immediately after the main shock. Friction laws, cascades of aftershocks and dynamical effects are not in the scope of this model but we agree that they may have an impact on the aftershock sequence [*Dieterich*, 1994; *Ogata*, 1999; *Sornette and Sornette*, 1999]. The purpose of this article is to underline different possible behaviors related to the aftershock temporal distribution, and, it is a chance that such behaviors can be approached by a restricted formalism based on physical principle. The selection of only few aftershock sequences

Table 6. Transient Regime Toward an Exponential Decay Rate of the Aftershock Sequence of the BN Nuclear Test and Comparisons Between the LPL and the MOL[a]

M_{min}	N	$10^3\,\lambda_a$	λ_b	$t_1^{0.8}$	$t_2^{0.8}$	q	p	c	Δ_{AIC}
				LPL				MOL	
			BN Nuclear Test (19 December 1968; $T_{start} = 2 \times 10^{-4}$ days, $T_{stop} = 134.8$ days)						
1.7	935	24	1.99	0.23	0.14	0.30	2.00	8.88	−13.69
1.9	842	25	1.35	0.50	0.67	0.42	2.11	8.95	−15.60
2.1	680	26	1.45	0.56	1.20	0.49	2.02	7.13	−16.31
2.3	524	32	2.38	0.27	0.40	0.40	2.11	6.70	−16.23
2.5	366	40	*	*	0.04	0.26	2.17	5.69	−19.70
2.7	240	40	*	*	0.20	0.36	1.91	3.49	−27.88
2.9	162	37	*	*	0.55	0.44	1.65	1.94	24.28

[a]N is the number of aftershocks for the minimum magnitude M_{min}. The star symbols indicate that our estimations of λ_a are equal to the lowest value allowed by our computations (10^{-9}). λ_a and λ_b have units of d^{-1}, $t_1^{0.8}$, $t_2^{0.8}$, and c have units of days, and q and p are unitless. Δ_{AIC} is the difference between the AICs of the LPL.

for analysis means that the empirical support provided for the model has still to be improved and we now plan to extend our study to a large suit of aftershock sequences. On the other hand, direct simulations done via a multiscale cellular automaton confirm the theoretical results presented in this work [*Narteau et al.*, 2000].

[45] Our model is consistent with the data, and, in almost all cases examined here, it outperforms the MOL hypothesis despite a penalty for the extra parameter. Specifically, it seems to capture essential aftershock behaviors not only over shortest and longest times but also during the transition from one regime to another.

[46] In our model, the power law decay is limited over short and large times by characteristic aftershock rates, λ_a and λ_b. Then, if λ_a and λ_b are 0 and infinity respectively, the aftershock decay rate is hyperbolic with respect to the exponent q. q and λ_a act as p and c in the MOL (1), while over long times the λ_b value can be associated to a transient time of an exponential decay. Consequently, if $\lambda_a \to 0$ and $p = q$, c can be derived from λ_b to make (1) and (5) equal. Because λ_a and λ_b may converge to each other, the aftershock decay rate can take many different forms but the final stage is always an exponential decay. We showed that such a diversity may be observed in real aftershock sequences and we therefore maintain that our model of aftershock decay rate complements the MOL. Furthermore, this richer class of behaviors is obtain through physical assumptions which can give a deeper understanding of the genesis of the aftershock sequence.

[47] This model is not empirical, it approximates characteristic timescale from a time-dependent law and a schematic state of stress within the fault zone. Consequently q, λ_a and λ_b can be associated with physical parameters as summarized below.

[48] Theoretically, the magnitude of q is determined by the shape of the time-dependent law and the shape of the overload distribution (Figure 1, columns 1 and 2). Steeper slopes of these relationships correspond to lower magnitudes of the q value. Thus, q reflects not only the complexity of the overload distribution resulting from the stress perturbation and the preexisting stress but also the internal acceleration process leading to the rupture. It can explain not only the range of power law decay reported in the literature (0.9–1.5 according to *Utsu et al.* [1995]) but also the spatial variability of the p value in an aftershock zone [*Wiemer and Katsumata*, 1999]. In our model, because the power law decay is limited in time, we propose a larger range of q value from 0.3 to 1.9. In general, the q value is lower than the p value and lower than 1. The transition toward an exponential aftershock decay rate over long times may explain the difference between the q and the p values but it definitely limits the number of aftershocks. Some sort of transition is surely inevitable for any event with $p < 1$, since otherwise an infinite number of aftershocks would eventually occur.

[49] The characteristic rate λ_b determines the lowest timescale of the aftershock sequence and it may be related to the rupture duration. The magnitude of this characteristic rate is associated with the highest magnitude of the overload just after the main shock. Because it simultaneously reflects the absolute crustal strength and the highest stress perturbation produced by the main shock, only the combined effect of these two factors can be inferred.

[50] The characteristic rate λ_a determines the largest timescale of the aftershock sequence. The magnitude of λ_a approximates the acceleration of the fracturing process at the threshold under which the strengthening process dominates and prevents the initiation of the rupture. From different examples, we have related this rate to the structural scale of faulting and the complexity of the fault network, notably its correlation length. For this reason, λ_a^{-1} can be referred to as a correlation time.

[51] The temporal limits of the power law aftershock decay rate can be derived from λ_a and λ_b. The comparison between these temporal limits and independent geophysical observations provides different pieces of evidence in order to describe more general aftershock sequence properties.

[52] When it is not an artifact, it is assumed in this paper that the onset of the power law aftershock decay rate is delayed according to a decreasing magnitude of the zones of highest overload. A lack of such zones may be associated with (1) the earthquake recurrence time and fault interactions, (2) the weakening process related to the deformation rate along faults, (3) the regularity of the rupture, and (4) the heat flow and the pore pressure. Therefore, we suggest that short recurrence times, regular faults and high deformation rates are good indicators of large c value ($\sim t_1$). Nevertheless, most of the time, as for example for the IV aftershock sequence, it is more likely a combination of these different factors which can explain the origin of the magnitude of the c value ($\sim t_1$). To differentiate between these factors, we plan to study the first stages of other aftershock sequences, and particularly these produced by similar rupture patterns, if possible along the same fault.

[53] The concept that the aftershock sequence properties may be related to the network of existing fractures has been suggested from laboratory tests by *Hirata* [1987]. In a sample of basalt under uniaxial compression, he recorded successive bursts of acoustic emissions and extracted from them main shock–aftershocks sequences. Following the advances of the fracturing process, he argued that the aftershock decay rates operates a transition from an exponential decay ($\sim\exp(-pt)$) to an Omori's power law decay (1) and that the p value continuously decreases. From geomorphological analysis and measurements of the fractal dimension of the fault system in aftershock regions, *Nanjo et al.* [1998] also find that the p value decrease with time according to the development of the fault network.

[54] Our results appear to verify that the preexisting fault network controls some characteristics of the aftershock decay rate. More exactly, we have observed that the strain rates, and both the shape and the complexity of the fault networks affect the aftershock frequency at which the exponential decay dominates the power law decay. This frequency decreases according to an increasing complexity of the fault network. Then, aftershock regions at the boundary between larger fault systems and zones under low strain rates exhibit a higher aftershock rate when the exponential decay appears. If the correlation time is less that 2 days, then the power law decay can not be seen.

[55] From our study and previous modeling [*Narteau et al.*, 2000], we conclude that the concentration of the deformation along major faults and the emergence of a dominant faulting mechanism both decrease the amplitude of λ_b. Then, following the evolution of the fault network [*Cowie*, 1998;
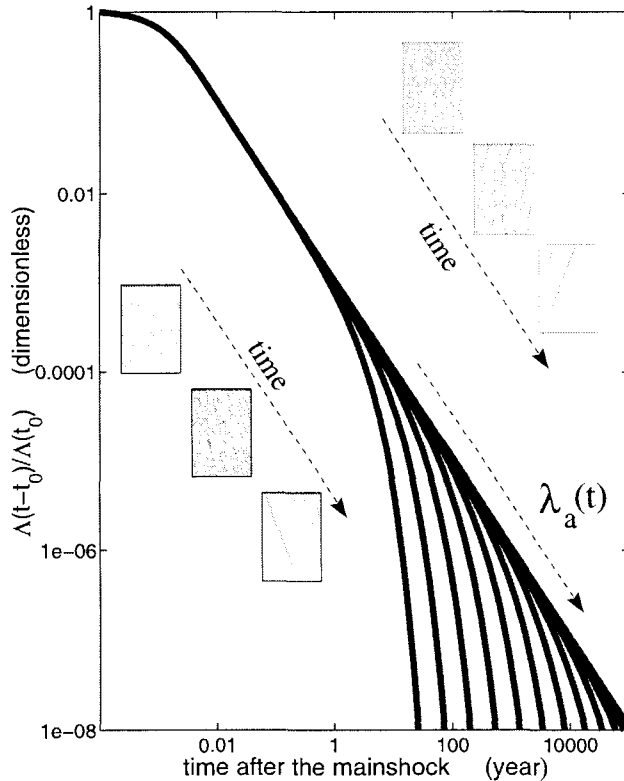
Figure 4. Schematic representation of a possible evolution of the aftershock decay rate through time according to the evolution of fault network. The curves represent (5) with $A = 1$, $\lambda_a = 10^3$, $q = 1$, and λ_b varying from 1 to 10^{-7} in logarithmic steps. The insets represent fault networks at different times. The lower insets represent the evolution of a dextral strike-slip fault network, while the upper one represents the evolution of a network of conjugate strike slip fault (Narteau, submitted manuscript, 2002).

C. Narteau, Formation and evolution of a population of strike-slip faults in a multiscale cellular automation model, submitted to *Geophysical Journal International*, 2002, hereinafter referred to as Narteau, submitted manuscript, 2002], the power law decay phase dominates the aftershock decay rate over larger and larger time periods. Even if we have not enough indices to distinguish any change of the p value, we argue that our observations are one step further the observations of *Hirata* [1987] and *Nanjo et al.* [1998]. We suggest that the exponential and the power law decay are permanently present and that the transition observed by *Hirata* [1987] only reflects the increase of the transient time associated with the exponential decay (Figure 4). The evolution of the p value also observed by *Nanjo et al.* [1998] may be only an artifact resulting from the estimate of the parameters of the MOL. Because the power law and the exponential tail are simultaneously present, the estimations should include both decay laws. Consequently, we propose to systematically test our model of aftershock decay rate in order to distinguish in time these different regimes.

[56] This paper has presented and discussed evidence that in aftershock sequences, the transient time of an exponential decay may be strongly related to the correlation length of the

preexisting fracture field (Figure 4). Such a relationship between a correlation time and a correlation length is common in the physics of critical phenomena. From this point of view, the variation that we suggest indicates that the aftershock regions are converging toward a critical point from a subcritical state. At this critical point, the correlation length–time is infinite. In our case, it corresponds to a permanent power law decay. This link between the earthquake physics and the critical phenomena physics has already been suggested by many authors [*Allègre et al.*, 1982], and the gamma function has been used under many different geophysical contexts in order to describe some spatial-temporal properties of the fracturing process [*Main*, 1996]. Here, we add another element to this growing body of evidence.

5. Conclusion

[57] In this study of the aftershock decay rate we first derived constitutive rules via a Markov process with stationary transition rates, and hence derived the magnitude of the exponent of the power law decay from different states of stress and different time-dependent behaviors. Analytical solutions for exponents q larger, equal and lower than 1 are presented. These analytical solutions use the same equation with different parameters, and we propose this equation as a general model of aftershock decay rate. In this model, the power law decay is limited in time by two characteristic rate constants. Over short times, a linear decay dominates while over long times an exponential decay dominates. Power law decay rates appear between these major regimes and if the characteristic rates are on the same order of magnitude, only an exponential decay may emerge over long times. Our model has a finite frequency at $t = 0$ and a convergent integral. Most of all, it incorporates physical assumptions which can be validated on real aftershock sequences and independent geophysical observations.

[58] From the comparison with real aftershock sequences, we show that, in almost all cases examined here, our model provides a better fit than the MOL. From the confrontations with independent physical observations, we conclude that the duration of the linear decay regime just after the main shock may be a consequence of the lack of zones of highest stress. Then, short repeat time and regular rupture are possible ingredients that prolong this initial regime. We also suggest that the duration of the power law decay phase increases with time as long as the strain concentrates on larger and larger faults with one particular type of faulting mechanism.

References

Akaike, H., A new look at the statistical model identification, *IEEE Trans. Autom. Control*, *AC-19*, 716–723, 1974.

Allègre, C. J., J. L. Le Mouël, and A. Provost, Scaling rules in rock fracture and possible implications for earthquake prediction, *Nature*, *297*, 47–49, 1982.

Astiz, L., and P. Shearer, Earthquake locations in the inner continental borderland, offshore southern California, *Bull. Seismol. Soc. Am.*, *90*, 425–449, 2000.

Atkinson, B. and P. Meredith, *The Theory of Subcritical Crack Growth With Applications to Minerals and Rocks*, Academic, San Diego, Calif., 1987.

Atkinson, B. K., Subcritical crack growth in geological materials, *J. Geophys. Res.*, *89*, 4077–4114, 1984.

Cowie, P., A healing-reloading feedback control on the growth rate of seismogenic faults, *J. Struct. Geol.*, *20*, 1075–1087, 1998.

Das, S., and C. Scholz, Theory of time-dependent rupture in the Earth, *J. Geophys. Res.*, *86*, 6039–6051, 1981.

Dieterich, J., A constitutive law for rate of earthquake production and its application to earthquake clustering, *J. Geophys. Res.*, *99*, 2601–2618, 1994.

Doser, D., A re-examination of the 1947 Manix, California earthquake sequence and comparison to other sequences within the Mojave block, *Bull. Seismol. Soc. Am.*, *80*, 267–277, 1990.

Gardner, J., and L. Knopoff, Is the sequence of earthquakes in southern California with aftershocks removed Poissonian?, *Bull. Seismol. Soc. Am.*, *5*, 1363–1367, 1974.

Gross, S., Aftershocks of nuclear explosions compared to natural aftershocks, *Bull. Seismol. Soc. Am.*, *86*, 1054–1060, 1996.

Gross, S., and C. Kisslinger, Tests of the models of aftershocks rate decay, *Bull. Seismol. Soc. Am.*, *84*, 1571–1579, 1994.

Hamilton, R., and J. Healy, Aftershocks of the Benham nuclear explosion, *Bull. Seismol. Soc. Am.*, *59*, 2271–2281, 1969.

Hauksson, E., and L. Jones, The July 1986 Oceanside M_L = 5.3 earthquake sequence in the continental borderland, southern California, *Bull. Seismol. Soc. Am.*, *78*, 1885–1906, 1988.

Hauksson, E., et. al., The 1999 MW 7.1 Hector Mine, California earthquake sequence: Complex conjugate strike-slip faulting, *Bull. Seismol. Soc. Am.*, *92*, 1154–1170, 2002.

Hauksson, E., and L. Jones, The 1992 Landers earthquake sequence: Seismological observations, *J. Geophys. Res.*, *98*, 19,835–19,858, 1993.

Hirata, T., Omori's power law aftershock sequences of microfracturing in rock fracture experiment, *J. Geophys. Res.*, *92*, 6215–6221, 1987.

Kisslinger, C., The stretched exponential function as an alternative model for aftershock decay rate, *J. Geophys. Res.*, *98*, 2271–2281, 1993.

Kisslinger, C., Aftershocks and properties of fault zones, in *Advances in Geophysics*, edited by R. Dwomska, pp. 1–36, Academic, San Diego, Calif., 1996.

Kisslinger, C., and L. Jones, Properties of aftershocks in southern California, *J. Geophys. Res.*, *96*, 11,947–11,958, 1991.

Knopoff, L., The magnitude distribution of declustered earthquakes in southern California, *Proc. Natl. Acad. Sci. U.S.A.*, *97*, 11,880–11,884, 2000.

Lachenbruch, A., J. Sass, and S. Galnis, Heat flow in southernmost California and the origin of the Salton Trough, *J. Geophys. Res.*, *90*, 6709–6736, 1985.

Lawn, B. and T. Wilshaw, *Fracture of Brittle Solids*, Cambridge Univ. Press, New York, 1975.

Main, I., Applicability of time-to-failure analysis to accelerated strain before earthquakes and volcanic eruptions, *Geophys. J. Int.*, *139*, F1–F6, 1999.

Main, I. G., Statistical physics, seismogenic, and seismic hazard, *Rev. Geophys.*, *34*, 433–462, 1996.

Mogi, K., Earthquakes and fractures, *Tectonophysics*, *5*, 35–55, 1967.

Nanjo, K., H. Nagahama, and M. Satomura, Rates of aftershock decay and the fractal structure of active fault systems, *Tectonophysics*, *287*, 173–186, 1998.

Narteau, C., P. Shebalin, M. Holschneider, J. L. Le Mouël, and C. J. Allègre, Direct simulation of the stress redistribution in the scaling organization of fracture tectonics, *Geophys. J. Int.*, *141*, 115–135, 2000.

Nyffenegger, P., and C. Frohlich, Recommendations for determining p values for aftershock sequences and catalogs, *Bull. Seismol. Soc. Am.*, *88*, 1144–1154, 1998.

Ogata, Y., Estimation of the parameters in the modified Omori formula for aftershocks frequencies by a maximum likelihood procedure, *J. Phys. Earth*, *31*, 115–124, 1983.

Ogata, Y., Seismicity analysis through point-process modeling: A review, *Pure Appl. Geophys.*, *155*, 471–508, 1999.

Omori, F., On after-shocks of earthquakes, *J. Coll. Sci., Imp. Univ. Tokyo*, *7*, 111–200, 1894.

Otsuka, M., Physical interpretation of Omori's formula, *Sci. Rep. Shimabara Earthquake Volcano Obs.*, *13*, 11–20, 1985.

Pacheco, J., and J. Nábělek, Source mechanisms of three moderate Californian earthquakes of July 1986, *Bull. Seismol. Soc. Am.*, *78*, 1907–1929, 1988.

Phillips, W. S., D. C. Pearson, X. Yang, and B. Stump, Aftershocks of an explosively induced mine collapse at White Pine, Michigan, *Bull. Seismol. Soc. Am.*, *89*, 1575–1590, 1999.

Press, W. H., S. A. Teulosky, W. T. Vetterling, and B. P. Flannery, *Numerical Recipes in C*, Cambridge Univ. Press, New York, 1992.

Ron, H., G. Beroza, and A. Nur, Simple model explains complex faulting, *Eos*, *82*, 128–129, 2001.

Scholz, C., Microfractures, aftershocks, and seismicity, *Bull. Seismol. Soc. Am.*, *58*, 1117–1130, 1968a.

Scholz, C., The frequency–magnitude relation of microfracturing in rocks and its relation to earthquakes, *Bull. Seismol. Soc. Am.*, *58*, 399–415, 1968b.

Shaw, B., Generalized Omori law for aftershocks and foreshocks from a simple dynamics, *Geophys. Res. Lett.*, *20*, 907–910, 1993.

Sieh, K., The repetition of large earthquake ruptures, *Proc. Natl. Acad. Sci. U.S.A.*, *93*, 3764–3771, 1996.

Sornette, D., and A. Sornette, Renormalization of earthquake aftershocks, *Geophys. Res. Lett.*, *26*, 1981–1984, 1999.

U.S.G.S., and C.D.M.G, Preliminary report on the 16 October 1999 M7.1 Hector Mine earthquake, *Seismol. Res. Lett.*, *71*, 11–23, 2000.

Utsu, T., A statistical study on the occurrence of aftershocks, *Geophys. Mag.*, *30*, 521–605, 1961.

Utsu, T., Y. Ogata, and R. Matsu'ura, The centenary of the Omori formula for a decay law of aftershocks activity, *J. Phys. Earth*, *43*, 1–33, 1995.

Webb, T., and H. Kanamori, Earthquake focal mechanisms in the eastern Transverse Ranges and San Emigdio Mountains, southern California and evidence for a regional decollement, *Bull. Seismol. Soc. Am.*, *75*, 737–757, 1985.

Wiemer, S., and K. Katsumata, Spatial variability of seismicity parameters in aftershock zones, *J. Geophys. Res.*, *104*, 13,135–13,151, 1999.

Weimer, S., et al., Properties of the aftershock sequence of the 1999 MW 7.1 Hector Mine earthquake: Implications for aftershock hazard, *Bull. Seismol. Soc. Am.*, *92*, 1227–1240, 2002.

Yamakawa, N., Foreshocks, aftershocks and earthquakes swarms, 4, Frequency decrease of after shocks in its initial and later stages, *Pap. Meteorol. Geophys.*, *19*, 109–119, 1968.

Yamashita, T., and L. Knopoff, Models of aftershocks occurrence, *Geophys. J. R. Astron. Soc.*, *91*, 13–26, 1987.

———————————————

M. Holschneider, Applied and Industrial Mathematics, University of Potsdam, PF 60 15 53, D-14415, Potsdam, Germany. (hols@math.uni-potsdam.de)

C. Narteau, Geology and Geophysics, Grant Institute, University of Edinburgh, West Mains Road, Edinburgh, EH9 3JW, UK. (Clement. Narteau@glgl.ed.ac.uk)

P. Shebalin, International Institute of Earthquake Prediction Theory and Mathematical Geophysics, Warshavskoye shosse, 79, korp 2, Moscow, 113556, Russia. (shebalin@mitp.ru)